

Article

Tubulin Polyglutamylation by TTL1 and TTL7 Regulate Glutamate Concentration in the Mice Brain

Yashuang Ping^{1†}, Kenji Ohata^{1,2†}, Kenji Kikushima^{1,3}, Takumi Sakamoto¹, Ariful Islam¹, Lili Xu¹, Hengsen Zhang¹, Bin Chen¹, Jing Yan¹, Fumihito Eto¹, Chiho Nakane¹, Keizo Takao^{4,5}, Tsuyoshi Miyakawa^{5,6}, Katsuya Kabashima¹, Miho Watanabe⁷, Tomoaki Kahyo^{1,3}, Ikuko Yao^{1,3,8}, Atsuo Fukuda⁷, Koji Ikegami^{1,9}, Yoshiyuki Konishi^{1,10}, Mitsutoshi Setou^{1,3,11,*}

¹ Department of Cellular and Molecular Anatomy, Hamamatsu University School of Medicine, 1-20-1 Handayama, Higashi-ku, Hamamatsu, Shizuoka 431-3192, Japan

² Department of Gastroenterology, Graduate School of Medicine, The University of Tokyo, 7-3-1 Hongo, Bunkyo-ku, Tokyo 113-0033, Japan

³ International Mass Imaging Center, Hamamatsu University School of Medicine, Hamamatsu, 1-20-1 Handayama, Higashi-ku, Hamamatsu, Shizuoka 431-3192, Japan

⁴ Department of Behavioral Physiology, Faculty of Medicine, University of Toyama, 2630 Sugitani, Toyama-shi, Toyama 930-0194, Japan

⁵ Genetic Engineering and Functional Genomics Unit, Frontier Technology Center, Graduate School of Medicine, Kyoto University, Kyoto 606-8501, Japan

⁶ Institute for Comprehensive Medical Science Division of Systems Medicine, Fujita Health University, Aichi 470-1192, Japan

⁷ Department of Neurophysiology, Hamamatsu University School of Medicine, Hamamatsu, 1-20-1 Handayama, Higashi-ku, Hamamatsu, Shizuoka 431-3192, Japan

⁸ Department of Biomedical Sciences, School of Biological and Environmental Sciences, Kwansei Gakuin University, 1 Gakuen Uegahara, Sanda, Hyogo 669-1330, Japan

⁹ Department of Anatomy and Developmental Biology, Graduate School of Biomedical and Health Sciences, Hiroshima University, 1-2-3 Kasumi, Hiroshima 734-8553, Japan

¹⁰ Department of Applied Chemistry and Biotechnology, University of Fukui, 3-9-1 Bunkyo, Fukui-shi, Fukui 910-8507, Japan

¹¹ Department of Systems Molecular Anatomy, Institute for Medical Photonics Research, Preeminent Medical Photonics Education & Research Center, 1-20-1 Handayama, Higashi-ku, Hamamatsu, Shizuoka 431-3192, Japan

* Correspondence: setou@hama-med.ac.jp; Tel.: +81-053-435-2086; Fax: +81-053-435-2468

† These authors contributed equally to this work.

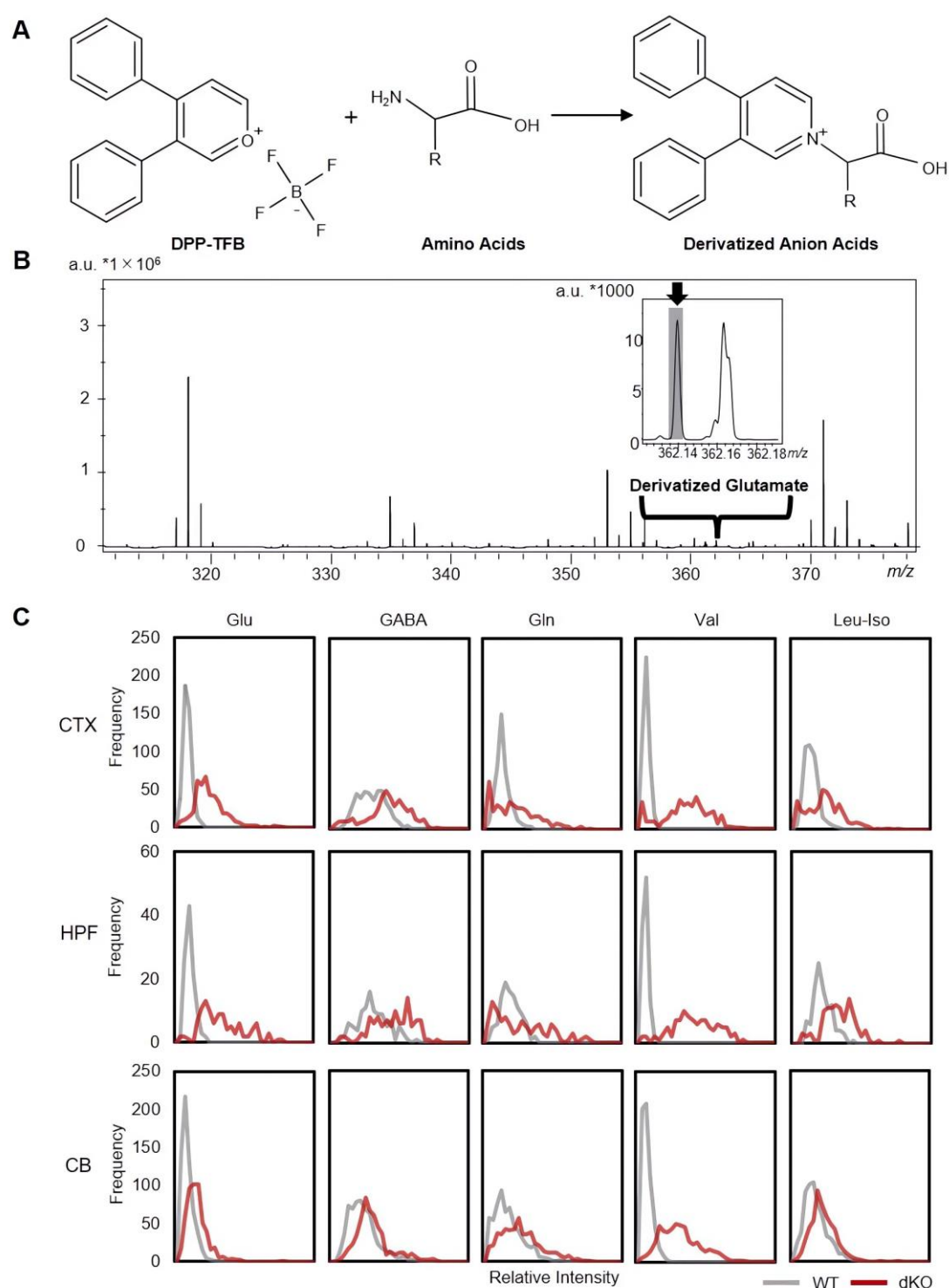


Figure S1. The derivatization of free amino acids by DPP-TFB and the relative intensity line graph of amino acid in the sagittal brain of mice sagittal brain. **(A)** Scheme of the derivatization of free amino acids by DPP-TFB. **(B)** The signal intensity of derivatized glutamate in brain tissues. **(C)** The frequency of the relative intensity of each spot in the selected regions of *Ttll1/Ttll7* double knockout and WT mice brains are represented in line graphs. Abbreviations: Glu: glutamate; GABA: γ -aminobutyric acid; Gln: glutamine; Val: valine; Leu-Iso: leucine-isoleucine; dKO: *Ttll1/Ttll7* double knockout.

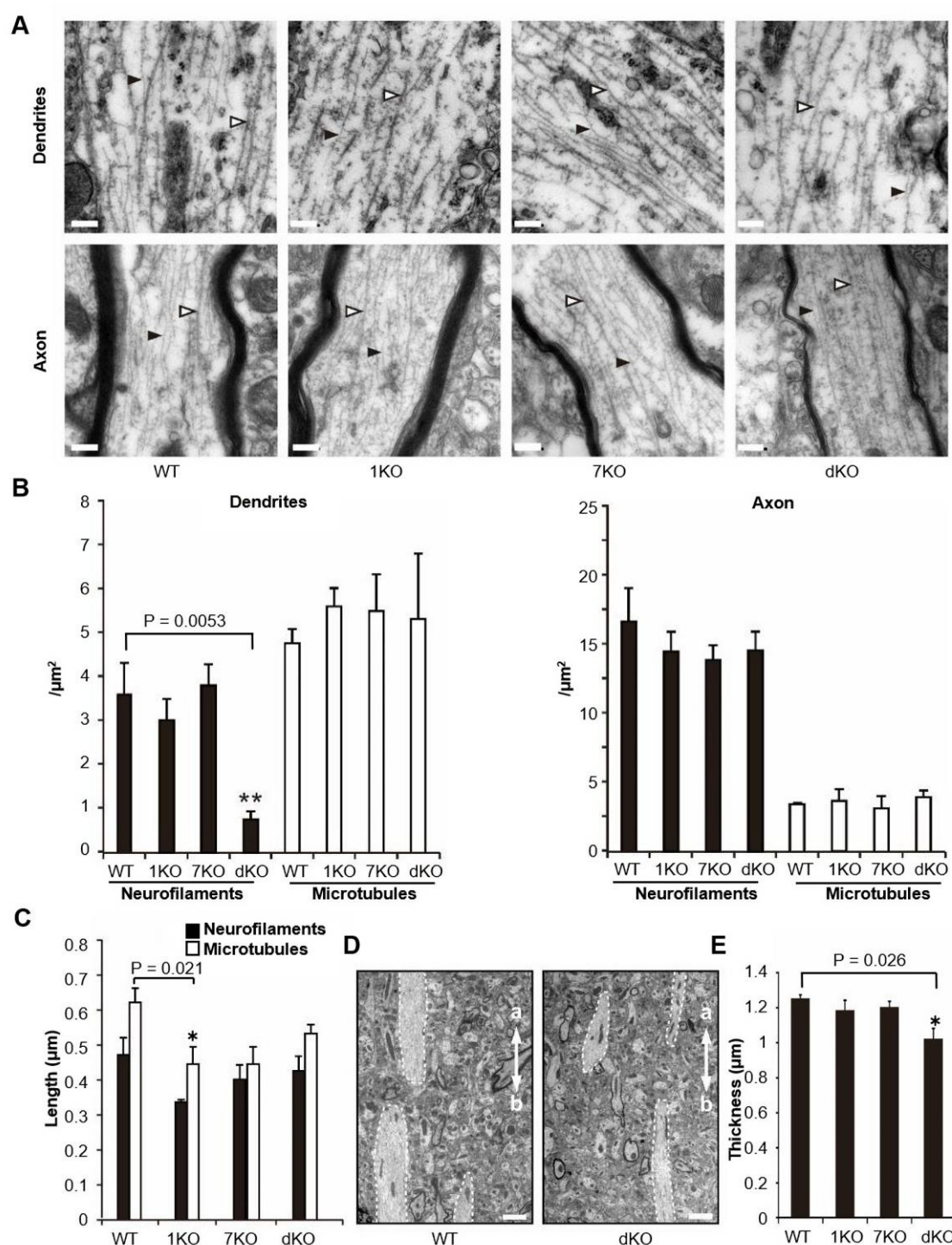


Figure S2. Electron microscopic observation of neurofilaments and microtubules in axons and dendrites of *Tll1* knockout mice. **(A)** Electron microscopic images of dendrites and axons from each transgenic mouse. Microtubules are pointed by white arrowheads, and neurofilaments are indicated by black arrowheads. Scale bars: 0.2 μm . **(B)** Densities of neurofilaments and microtubules in dendrites or axons were counted from the microscopic images of the cerebral cortex at layer II/III from each transgenic mouse. $p < 0.01$, denoted by **, (WT: 7 axons, 9 dendrites, $n = 4$ mice; 1KO: 7 axons, 6 dendrites, $n = 3$ mice; 7KO: 6 axons, 10 dendrites, $n = 3$ mice; dKO: 8 axons, 15 dendrites, $n = 4$ mice). **(C)** Neurofilament and microtubule lengths were calculated from EM images. $p < 0.05$, denoted by *. **(D)** Images of the dendritic shafts from wild type and *Tll1/Tll7* double knockout mice. Dendrites regions are indicated by dashed lines and measured at the widest region. a: apical direction; b: basal direction. Scale bar 2 μm . **(E)** The thickness of dendritic shafts from *Tll1/Tll7* double knockout mice was significantly reduced with $p < 0.05$, denoted by * (WT: 111 dendritic shafts, $n = 3$

mice; 1KO: 127 dendritic shafts, $n = 3$ mice; 7KO: 116 dendritic shafts, $n = 3$ mice; dKO: 132 dendritic shafts, $n = 3$ mice). Data represented as mean \pm SD in B, C, F, ANOVA followed by Dunnett's test. Abbreviations: 1KO: *Till1* knockout; 7KO: *Till7* knockout; dKO: *Till1/Till7* double knockout.

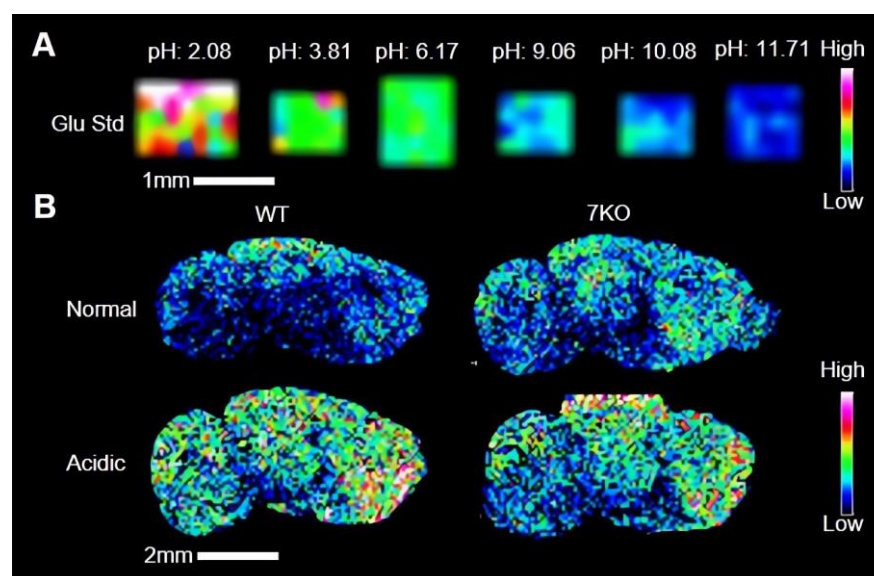


Figure S3. The detection efficiency of MALDI IMS for glutamate was influenced by pH. **(A)** Glutamate standard at different pH were detected by MALDI IMS, and the signal intensity of glutamate standards decreased with increasing pH. **(B)** Under normal conditions, glutamate concentrations in the brain of *Till7* knockout mice were higher than WT, but similar under acidic conditions. Abbreviations: Glu Std: Glutamate standard; 7KO: *Till7* knockout.

Table S1. MRM transitions and MS parameters for the analytes and IS of 4000 QTRAP MS/MS system.

Analyte	Precursor ion (m/z)	Product ion (m/z)	DP (V)	EP (V)	CE (V)	CXP (V)
Glu	148.1	84.0	26	10	21	12
IS-Glu	154.2	89.1	46	10	25	12
DPP-Glu	362.1	231.8	106	10	39	16
DPP-IS-Glu	368.1	232.9	46	10	35	8

MRM transitions and MS parameters for the analytes and IS of 4000 QTRAP MS/MS system. Abbreviations: Glu: glutamate, IS-Glu internal standard glutamate, DPP-Glu: DPP-TFB derivatization glutamate, DPP-IS-Glu: DPP-TFB derivatization internal standard glutamate, DP: declustering potential, EP: entrance potential, CE: collision energy, CXP: collision cell exit potential.